Measurement of Plasma Parameters in an Inductively Coupled Plasma Reactor

Hiroshi Sasaki, Kenichi Nanbu and Masayoshi Takahashi

Institute of Fluid Science, Tohoku University, Sendai, Japan 980-8577

Abstract. The objective is to deepen the understanding of basic plasma properties in a high-density inductively coupled plasma(ICP) reactor. The experiment using a Langmuir probe, which is made of tungsten wire having length of 2.3 mm and diameter of 0.65 mm, is carried out to determine the characteristics of argon plasma. The axial and radial distributions of the plasma density, electron temperature, and plasma potential are measured. It was found that the electron density is in the range of 1.0×10^{10} to $1.0\times10^{11}\,\mathrm{cm}^{-3}$, electron temperature $4\sim6$ eV, and plasma potential $35\sim45$ V, respectively. These plasma parameters are spatially nonuniform in the axial direction; they depend on the distance between the plasma source and the measuring point. Next, etching of polycristalline silicon wafer by chlorine plasma is studied. The results obtained in this study indicate the effects of rf coil power, gas pressure, and substrate rf bias power on the distributions of the etch rate.

INTRODUCTION

The size of microscopic features on electronic devices is becoming smaller and smaller whereas the size of wafers is becoming larger and larger to get more chips from one wafer. Increase in wafer size requires opening new fabrication facilities [1]. Plasma etching technology is highly expected to be much more advanced. Until quite recently, the development of etching technologies is mainly conducted based on experiences and limited measurements of basic plasma properties. However, in a near future such a stance will be confronted with a difficulty in the design of advanced etching apparatuses.

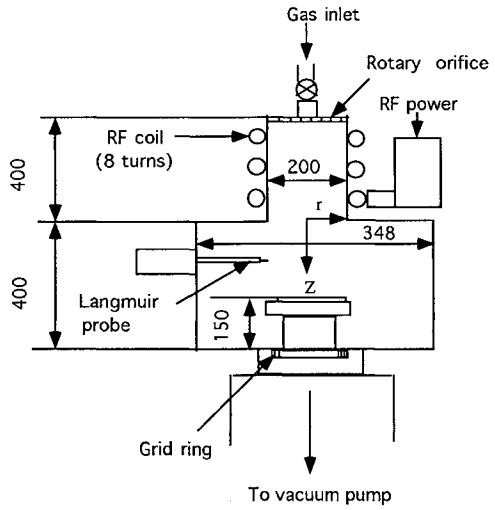

FIGURE 1. Schematic of ICP reactor.

TABLE 1. Measuring positions. The origin $z = 0$ is at the top of the diffusion chamber, whose height H is 400 mm.

Port No.	z(mm)	z/H
11	200	0.500
10	210	0.525
8	230	0.575
6	250	0.625
4	270	0.675
2	290	0.725

CP585, *Rarefied Gas Dynamics: 22nd International Symposium*, edited by T. J. Bartel and M. A. Gallis

REPORT DOCUMENTATION PAGE

Form Approved OMB No. 0704-0188

1. REPORT DATE (DD-MM-YYYY)	2. REPORT TYPE	3. DATES COVERED (FROM - TO)
09-07-2000	Conference Proceedings	09-07-2000 to 14-07-2000

4. TITLE AND SUBTITLE
Measurement of Plasma Parameters in an Inductively Coupled Plasma Reactor
Unclassified

5a. CONTRACT NUMBER
5b. GRANT NUMBER
5c. PROGRAM ELEMENT NUMBER

6. AUTHOR(S)
Sasaki, Hiroshi ;
Nanbu, Kenichi ;
Takahashi, Masayoshi ;

5d. PROJECT NUMBER
5e. TASK NUMBER
5f. WORK UNIT NUMBER

7. PERFORMING ORGANIZATION NAME AND ADDRESS
Institute of Fluid Science
Tohoku University
Sendai, Japan980-8577

8. PERFORMING ORGANIZATION REPORT NUMBER

9. SPONSORING/MONITORING AGENCY NAME AND ADDRESS
AOARD
Unit 45002
APO AP, xx96337-5002

10. SPONSOR/MONITOR'S ACRONYM(S)
11. SPONSOR/MONITOR'S REPORT NUMBER(S)

12. DISTRIBUTION/AVAILABILITY STATEMENT
APUBLIC RELEASE
,

13. SUPPLEMENTARY NOTES
See Also ADM001341, Rarefied Gas Dynamics (RGD) 22nd International Symposium held in Sydney, Australia, 9-14 July 2000.

14. ABSTRACT
The objective is to deepen the understanding of basic plasma properties in a high-density inductively coupled plasma(ICP) reactor. The experiment using a Langmuir probe, which is made of tungsten wire having length of 2.3 mm and diameter of 0.65 mm, is carried out to determine the characteristics of argon plasma. The axial and radial distributions of the plasma density, electron temperature, and plasma potential are measured. It was found that the electron density is in the range of 1.0 x 1010 to 1.0 x 1011cm~3, electron temperature 4 ~ 6 eV, and plasma potential 35 ~ 45 V, respectively. These plasma parameters are spatially nonuniform in the axial direction; they depend on the distance between the plasma source and the measuring point. Next, etching of polycristalline silicon wafer by chlorine plasma is studied. The results obtained in this study indicate the effects of rf coil power, gas pressure, and substrate rf bias power on the distributions of the etch rate.

15. SUBJECT TERMS

16. SECURITY CLASSIFICATION OF:			17. LIMITATION OF ABSTRACT	18. NUMBER OF PAGES	19. NAME OF RESPONSIBLE PERSON
a. REPORT	b. ABSTRACT	c. THIS PAGE	Public Release	8	Fenster, Lynn lfenster@dtic.mil
Unclassified	Unclassified	Unclassified			19b. TELEPHONE NUMBER International Area Code Area Code Telephone Number 703767-9007 DSN 427-9007

In this work, an inductively coupled plasma, whose density is high even at lower gas pressure, is studied experimentally to clarify how radicals formed in the plasma diffuse and are transported to the wafer. In order to completely solve this problem, not only the experiment but also numerical analyse based on accurate particle modeling [4,6] may be necessary at the same time. First, we constructed an inductively coupled plasma reactor and examined the basic properties of argon plasma [7]. Next, we started studying the etching properties of polycrystalline silicon wafer by chlorine plasma. The effects of rf coil power, substrate rf bias power, gas pressure, and gas flow rate on the etch rate and its distribution are examined. A microwave interferometer and a surface profiler(Tencor) are used to measure the electron density and the etch rate, respectively.

EXPERIMENTAL

The schematic of the inductively coupled plasma reactor is shown in Fig.1. The origin of the coordinate system is at the center of the entrance to the diffusion chamber. Let the r-axis be in the radial direction and z-axis be in the direction of the downward normal at the entrance. The reactor consists of a plasma source chamber ($z < 0$), diffusion chamber ($z > 0$), pumping system, and radio–frequency (rf) power source. The plasma source chamber is made of a quartz tube having inner diameter of 200 mm and height of 400 mm. The diffusion chamber is made of a stainless steel having inner diameter of 348 mm and height of 400 mm. The pumping system is driven by a turbo-molecular pump (210ℓ/sec) and an oil-rotary pump (162ℓ/min). Before starting measurements the diffusion chamber is evacuated up to pressure of 2.0×10^{-5} Pa. The working pressure is in the range of 0.2 – 2.0 Pa. The quart tube is wound by 8–turns helical coil. The diameter of the helical coil is 242 mm and the length is 274 mm. The coil is cooled by water to suppress the heating. The maximal input rf power of the coil is 500 W and the frequency is 13.56 MHz. Argon or chlorine gas is fed to the plasma source chamber through a rotating disk with many orifices which works for supplying gas uniformly from the top of the source chamber. The rotating disk has diameter of 198 mm, thickness of 5 mm, and 1139 latticed orifices with diameter of 1 mm. It is rotated at a desired speed clockwise or counterclockwise. Maximal speed is ±32 rpm. An annular aluminum plate is installed between the diffusion chamber and the entrance of the pumping system to realize a spatially uniform pumping. On this plate 24 holes of diameter of 10 mm are drilled.

A movable substrate holder has diameter of 156 mm. It can be moved vertically by ±50 mm from the standard position ($z = 250$ mm). In this work the holder position is fixed at $z = 300$ mm. The diffusion chamber has 11 ports for insertion of the Langmuir probe and a pair of view-ports for a microwave interferometer. There is still one port for a quadrupole mass spectrometer. The Langmuir probe (PMT Inc.) made of tungsten wire has length of 2.3 mm and diameter of 0.65 mm. This probe has an rf choke-coil for removing the noise in the I–V curve due to the radio frequency. The plasma potential, electron density, and electron temperature are obtain from the I–V curve. The probe can be quickly moved by compressed air to an arbitrary radial location in the chamber. The 20 data in the radial direction ($r < 300$ mm) can be obtained in one shot of the probe. The required time is 200 msec. The vertical distributions of the plasma parameters are obtained by changing the probe inserting port. The positions of measuring points z and the positions normalized by diffusion chamber height($H = 400$ mm) z/H are given in Table 1. In the experiment, gas pressure is in the range of 0.5 – 2.0 Pa, gas flow rate 5 – 100 sccm, and rf coil power 100 – 500 W with 13.56 MHz. The bias power for the substrate holder applied for chlorine plasma is in the range of 30 – 100 W with the same frequency. Gas pressure control is necessary to examine the effects of pressure on the plasma parameters. A conductance gate valve is used for this purpose at a constant flow rate(20 sccm). The effects of the flow rate on the plasma parameters are also examined in the range of 20 – 100 sccm.

RESULTS AND DISCUSSION

A. Argon plasma

First we present the data for argon ICP. The electron density N_e, electron temperature T_e, and plasma potential V_p are plotted as a function of gas pressure in Fig.2. The conditions are: rf coil power is 300 W,

gas flow rate 20 sccm, and the measuring position $z = 230$ mm and $r \sim 0$. As is shown in Fig.2, the electron temperature decreases with increasing pressure from 5.5 eV at 0.5 Pa to 4.3 eV at 2.0 Pa. The decrease in the electron temperature is due to inelastic collisions at higher gas pressure. The electron density increases with increasing the gas pressure from $6.0 \times 10^{10}\text{cm}^{-3}$ at 0.5 Pa to $8.7 \times 10^{10}\text{cm}^{-3}$ at 2.0 Pa. The electron density is lower than that we expected. One of the reasons for lower plasma density is that the measured position is far from the plasma source chamber. Next, let us see the plasma potential. It decreases as the pressure increases. It is well-known that lower plasma potential and lower electron temperature are desirable in etching processes [2]. In this sense, higher gas pressure appears to be recommendable. Of course, the gas pressure should be as low as possible for successful high aspect ratio etching. Figure 3 shows the plasma potential, electron density, and electron temperature as a function of the rf coil power for 20 sccm and 1.0 Pa at $z/H = 0.575$. The rf power is the one applied to the matching network; reflected power is nearly 0 W. The plasma potential increases with the rf coil power from 37 V at 100 W to 47 V at 500 W. Such high potential is undesirable in etching. The electron density increases from $4 \times 10^{10}\text{cm}^{-3}$ at 100 W to $9 \times 10^{10}\text{cm}^{-3}$ at 500 W. The electron temperature also increases slightly from 4.6 eV at 100 W to 5.2 eV at 500 W as the rf coil power increases.

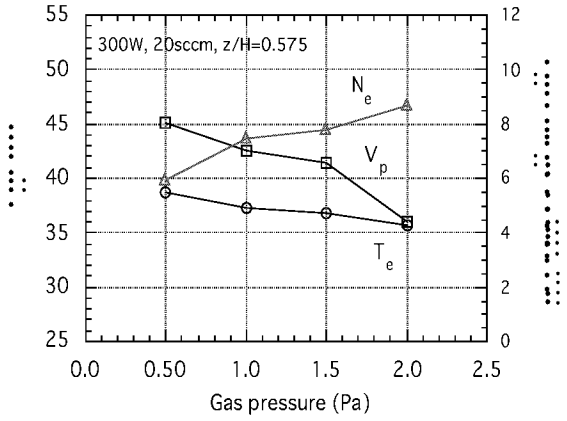

FIGURE 2. Electron density N_e, electron temperature T_e, and plasma potential V_p vs gas pressure.

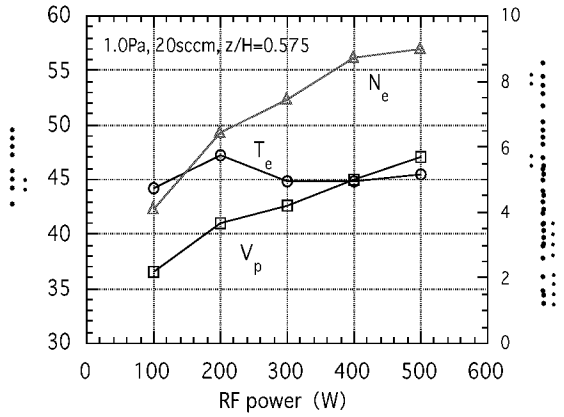

FIGURE 3. Plasma potential V_p, electron density N_e, and electron temperature T_e vs rf power.

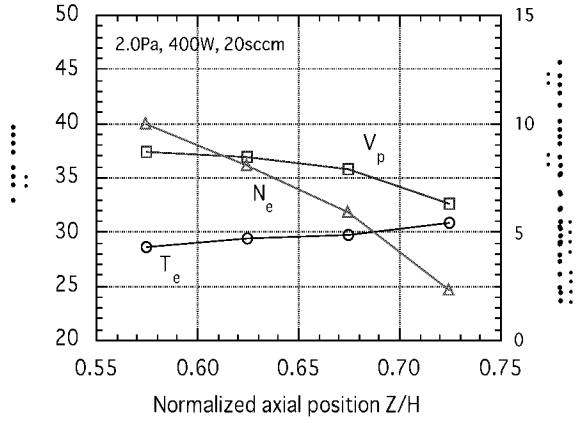

FIGURE 4. Axial distributions of plasma potential V_p, electron density N_e, and electron temperature T_e.

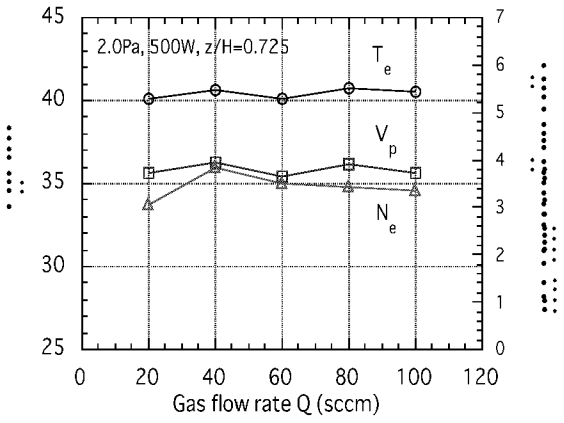

FIGURE 5. Plasma potential V_p, electron temperature T_e, and electron density N_e vs gas flow rate.

The axial distributions of the electron density, electron temperature, and plasma potential are shown in Fig.4. Experimental conditions are 2.0 Pa, 400 W, and 20 sccm. The normalized axial position, z/H, is measured downward from the entrance of the diffusion chamber. As is shown in Fig.4, the electron density decreases with increasing the axial position from $1.0 \times 10^{11}\text{cm}^{-3}$ at $z/H = 0.575$ to $2.3 \times 10^{10}\text{cm}^{-3}$ at $z/H = 0.725$. The main reason of this decrease is that electrons which reached the chamber wall by diffusion on the wall at the phase when the oscillating plasma potential is lowest. The plasma potential decreases from 37 V to 33 V and the electron temperature increases from 4.3 eV to 5.4 eV. Figure 5 shows the effect of gas flow rate on the plasma potential, electron density, and electron temperature at $z/H = 0.725$ for 2.0 Pa and 500 W. The plasma potential is nearly constant in the range of 20 – 100 sccm. The electron temperature and electron density are also nearly constant, 5.3 eV and $3.5 \times 10^{10}\text{cm}^{-3}$, respectively. We can see from Fig.5 that the change in the gas flow rate does not affect the plasma parameters very much. The electron density versus the normalized radial position, r/R, (R= 78 mm: radius of substrate holder) are shown in Fig.6. Experimental conditions are 0.5 Pa, 100 W, 20 sccm, and $z/H = 0.500 - 0.725$. Each profile is relatively uniform except the one at $z/H = 0.725$. This location is close to the substrate at $z/H = 0.750$. A good uniformity is due to a large coefficient near the center of the chamber in the case of low pressure discharge [3]. It is seen that the electron density at $z/H = 0.725$ rapidly decreases for $r/R < -0.8$. We suppose that this is caused by an asymmetrical pumping of gas. The electron density appears to be nearly the same in the range from $z/H = 0.500$ to 0.625, but as the axial distance increases more, the electron density decreases gradually.

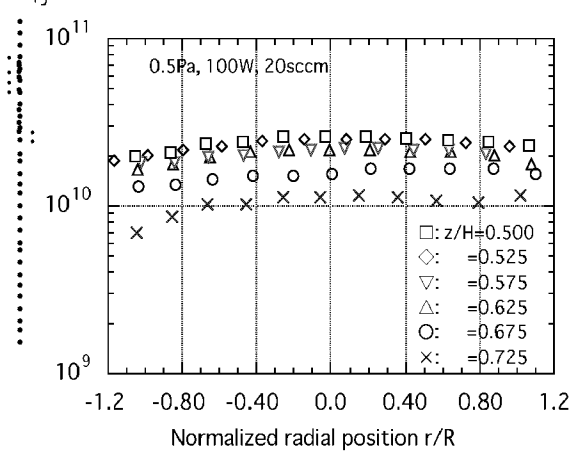

FIGURE 6. Radial distributions of electron density.

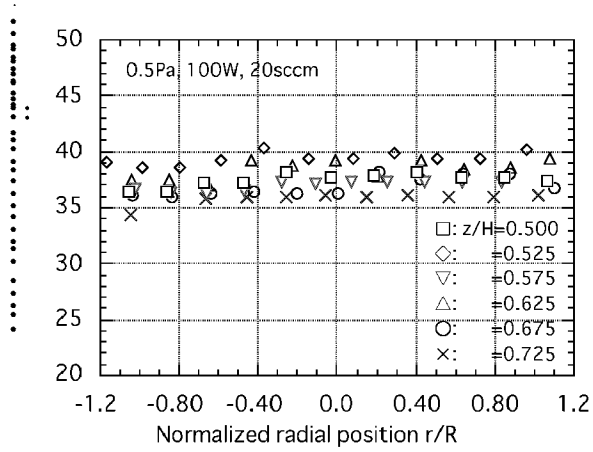

FIGURE 7. Radial distributions of plasma potential.

Figure 7 shows the radial distributions of the plasma potential under the same experimental conditions as that for Fig.6. The plasma potential is about 35 – 40 V in the range from $z/H = 0.500$ to 0.725. As the axial distance increases, the potential level decreases keeping the uniformity. The radial distributions of the electron temperature under the same conditions are shown in Fig.8. The electron temperature is 5 – 6 eV in the range of $z/H = 0.500 - 0.725$. The distributions are uniform in the radial direction.

The disk with the latticed orifices is rotated clockwise or counterclockwise at speed of ±20 rpm to see the effects of rotation on the plasma parameters. Figure 9 shows the electron density for ±20 rpm and 0 rpm. We see that the electron density distributions are very flat and uniform. It is reasonable to conclude that there is no effect of the rotation in the range of this disk speed. The radial distributions of the plasma potential and electron temperature are shown in Figs.10 and 11, respectively. Experimental conditions are the same as Fig.9. The distributions of the plasma potential and electron temperature are nearly flat, i.e. 38 V and 1.5 eV, respectively. Again there is no effect of the rotation. Consequently, we can say that Figs.9–11 give the error bound for our measurements. Note, however, that the effect of rotation did not improve the spatial uniformity because the latticed orifice already played a sufficient role for realizing the uniformity.

B. Silicon etching by chlorine plasma

We now discuss the etching properties of the silicon wafer by chlorine plasma. The diameter of the wafer is

152.4 mm. The wafer is set on the water-cooled substrate holder at the position of $z/H = 0.625$. The rf bias with the frequency of 13.56 MHz is applied to the holder. Figure 12 shows the relation between the etch depth and etching time near the center of the wafer. The etching conditions are as follows: Chlorine pressure is 0.5 Pa, RFC coil power 500 W, gas flow rate 20 scam, and rf substrate bias power 100 W. The etch depth increases linearly with time. The distributions of the etch rate of Si wafer are shown in Fig.13. The distance r from the center of the wafer along the $x-$and $y-$axis is the abscissa, where $xy-$plane is on the wafer. Measuring points are $r=$ 0 mm, ±20 mm, and ±40 mm in the two directions. Chlorine pressure is 0.5 Pa, rf coil power 500 W,

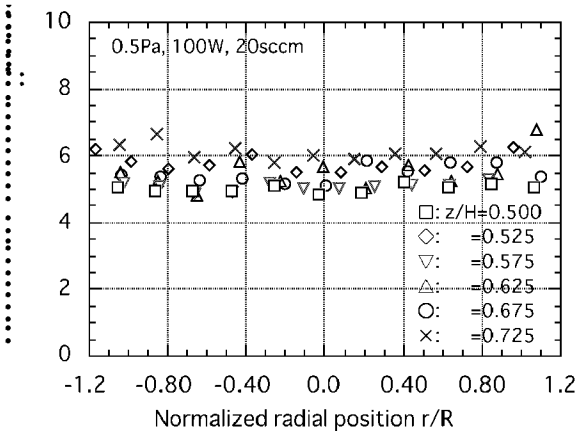

FIGURE 8. Radial distributions of electron temperature.

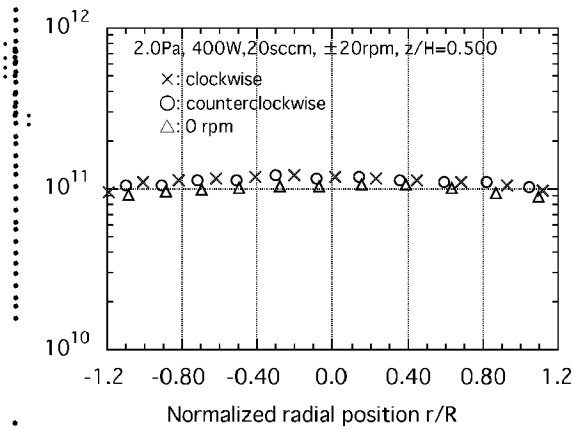

FIGURE 9. Effect of orifice rotation on radial distributions of electron density.

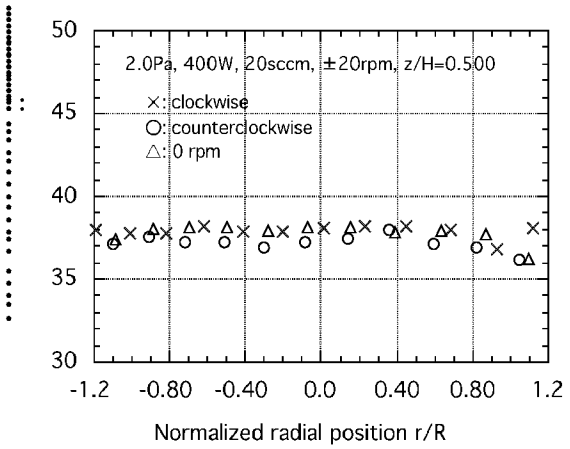

FIGURE 10. Effect of orifice rotation on radial distributions of plasma potential.

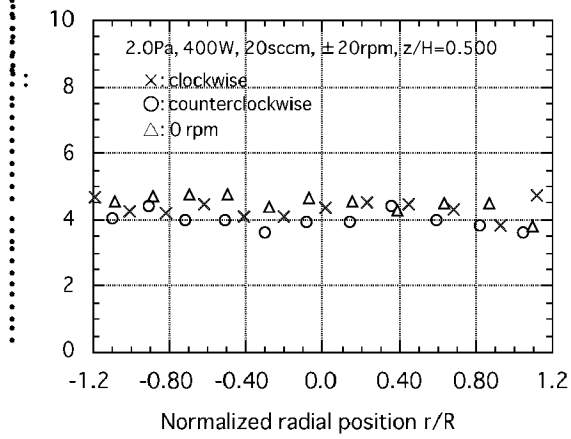

FIGURE 11. Effect of orifice rotation on radial distributions of electron temperature.

and gas flow rate 10 sccm. The etching time is five minutes. It is clear that the distributions of the etch rate are uniform. Figure 14 shows the changes in the etch rate and substrate peak-to-peak voltage V_{pp} with the rf coil power. The etch rate decreases rapidly with increasing the coil power in the regime of the rf coil power less than 300 W, beyond which the etch rate decreases very slowly with increasing the coil power. On the contrary, the substrate peak-to-peak voltage is unchanged in the regime less than 300 W and then V_{pp} decreases rapidly with a further increase of the power. Reflection on these suggests that the decrease of the etch rate is due to the reduction of the substrate peak-to-peak voltage. Next, the relation between the etch rate and the gas pressure is shown in Fig.15. The experimental conditions are as follows: Gas flow rate is 10 sccm, rf coil power 500 W, substrate bias power 50 W, and etching time five minutes. The etch rate increases with increasing gas

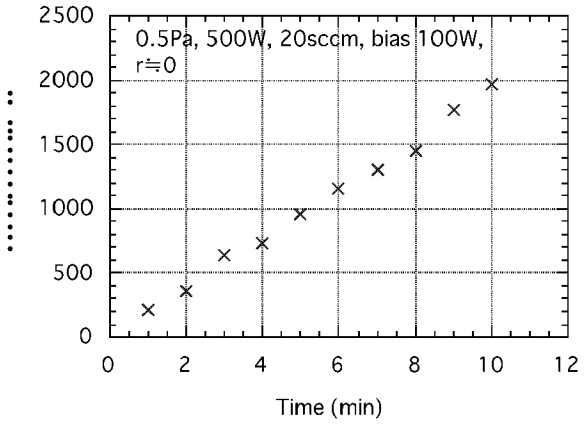

FIGURE 12. Relation between etch depth and etching time.

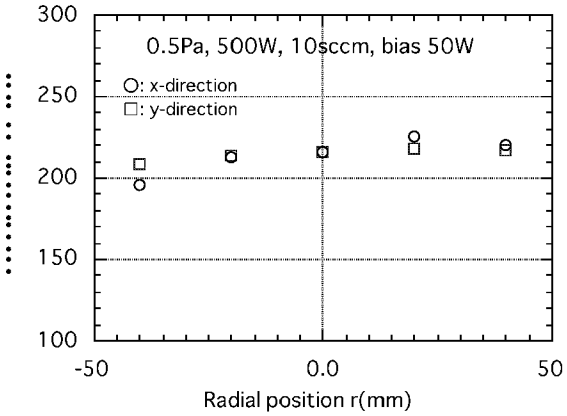

FIGURE 13. Distributions of the etch rate of Si wafer.

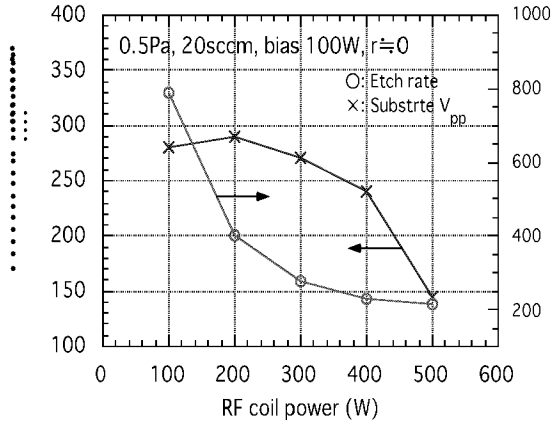

FIGURE 14. Changes in etch rate and substrate peak-to-peak voltage with rf coil power.

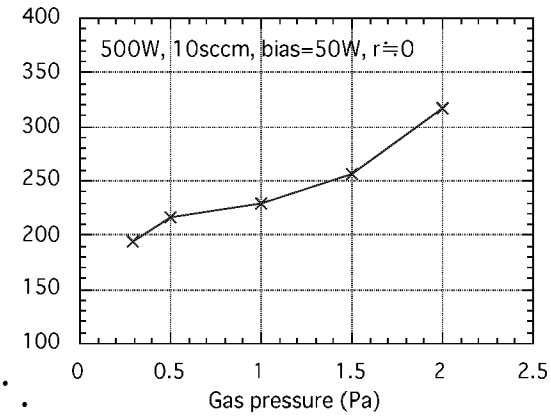

FIGURE 15. Relation between etch rate and gas pressure.

pressure. Roughly, the etch rate shows a linear increase. When the gas pressure becomes higher, the substrate peak-to-peak voltage increases due to the higher impedance of the plasma, which results in larger etch rate. The radial distributions of the etch rate are shown as a function of gas pressure in Fig.16. When the gas pressure is lower than 1.0 Pa, the distributions are nearly the same, therefore it can be said that there is no effect of gas pressure. However, when it is higher than 1.0 Pa, the etch rates increase with increasing gas pressure, and the distributions of the etch rate are not uniform. This is due to the collisions among the plasma particles in the chamber. Figure 17 shows the etch rate as a function of the substrate rf bias power. Gas pressure is 0.5 Pa, rf coil power 500 W, and gas flow rate 20 sccm in this case. The etch rate increases linearly as the rf bias power increases. The reason is that the energy of ions incident on the wafer increases with the rf bias power and hence the probability of surface reaction becomes larger with the bias power. Finally, the change in the electron density with time is measured when etching is going on. The electron density during etching is measured using the microwave interferometer. Figure 18 shows the change in the electron density with time for various gas pressure. Etching time is five minutes, rf coil power 500 W, gas flow rate 10 sccm, substrate rf bias power 50 W, and pressure is in the range of 0.5 – 2.0 Pa. As is shown in Fig.18, the electron density decreases with increasing gas pressure and also the electron density slightly changes with time. Next, the relation between the electron density and the rf coil power is plotted in Fig.19. It is clear that the electron

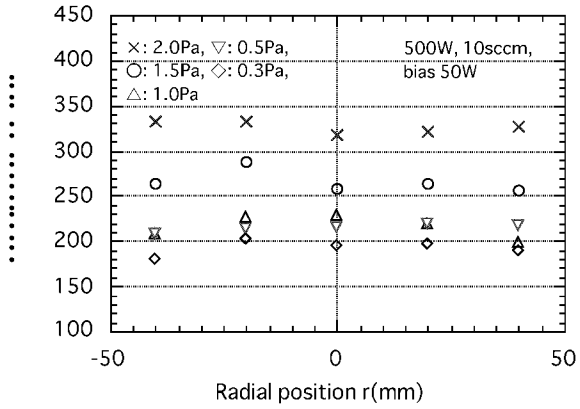

FIGURE 16. Radial distributions of etch rate of Si.

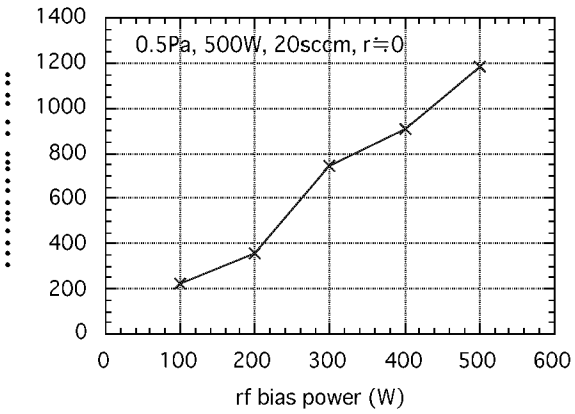

FIGURE 17. Etch rate of Si vs rf bias power.

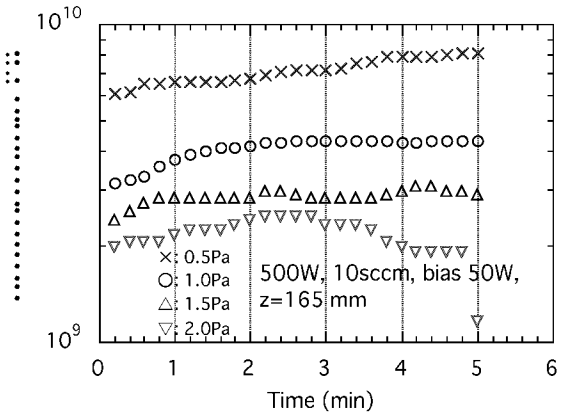

FIGURE 18. Relation between electron density and gas pressure.

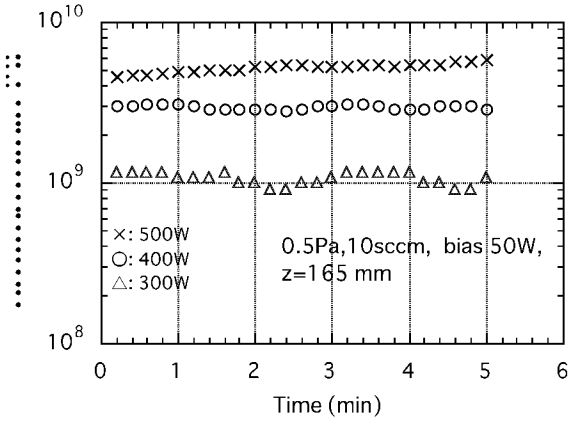

FIGURE 19. Relation between electron density and rf coil power.

density increases with rf coil power. The electron density changes with time. Figures 18 and 19 show that the state of plasma is stable in our reactor.

CONCLUSIONS

Basic plasma properties in the ICP reactor were systematically examined for argon discharge plasma using the Langmuir probe. Also, etching properties of polycrystalline silicon wafer in chlorine plasma were studied.

We clarified the dependence of plasma parameters on the gas pressure, the rf power, and the distance from the plasma source. The radial distributions of the plasma potential, electron temperature, and electron density were very uniform. As the gas pressure increases, the electron density increases but, the plasma potential and electron temperature decrease. Both the electron density and plasma potential increase with increasing the rf coil power but the electron temperature does not change. If we used the inlet disk with the latticed orifice, there is no need to rotate the orifice to realize a spatially uniform plasma. The gas flow rate has no effect on the plasma parameters in the range of 20 – 100 sccm. As the distance between the plasma source and the measuring point increases, the electron density and plasma potential decrease, whereas the electron temperature increases slightly.

As for chlorine plasma, the etch depth increases linearly with etching time. The electron density increases with the source (rf coil) power. Although the etch rate increases with the biasing power, it decreases with the rf coil power. The distribution of the etch rate of Si wafer was uniform in the ICP reactor.

REFERENCES

1. Flamm,D.L. and Herb,D.K., *Plasma Etching: An Introduction*, Eds.Manos,D.M. and Flamm,D.L., New York: Academic Press, 1989.
2. Hopwood,J., Guuarnieri,C.R., Whitehair,S.J., and Cuomo,J.J., Langmuir probe measurements of a radio frequency induction plasma. *J. Vac. Sci. Technol.* **A11**(1), 152-156(1993).
3. Hopwood, J., Review of inductively coupled plasmas for plasma processing. *Plasma Sources Sci. Technol.*, **1**, 109-116(1992).
4. Nanbu,K., Morimoto,T., and Suetani,M. Direct Simulation Monte Carlo analysis of flows and etch rate in an inductively coupled plasma reactor. *IEEE Trans.Plasma Sci.* **27**, 1379-1388(1999).
5. Nanbu,K., Suetani,M., and Sasaki,H. Direct Simulation Monte Carlo(DSMC) modeling of silicon etching in radio-frequency chlorine discharge. *Computational Fluid Dynamics Journal.* **8**, 257-265(1999).
6. Nanbu,K., Nakagome,T., and Kageyama,J. Detailed structure of the afterglow of radio-frequency chlorine discharge. *Jpn. J.Appl.Phys.* **38**, L951-L953 (1999).
7. Sasaki,H., Nanbu,K., and Takahashi,M. Basic plasma properties in a high-density ICP etching apparatus. *Proc. 17th Symp. Plasma Processing* (Nagasaki, Japan), 125-128(2000).